Reversible Self-Organization of Poly(ethylene glycol)-Based Hybrid Block Copolymers Mediated by a De Novo Four-Stranded α-Helical Coiled Coil Motif

Guido W. M. Vandermeulen,[†] Christos Tziatzios,[‡] and Harm-Anton Klok*[,†,§]

Max Planck Institute for Polymer Research, Ackermannweg 10, D-55128 Mainz, Germany, and Johann Wolfgang Goethe-Universität, Institut für Biophysik, Theodor-Stern-Kai 7, D-60590 Frankfurt am Main, Germany

Received January 30, 2003; Revised Manuscript Received April 4, 2003

ABSTRACT: This paper describes the synthesis and supramolecular organization of two novel hybrid diblock copolymers based on poly(ethylene glycol) (PEG) and peptide sequences inspired by the coiled coil protein folding motif. The self-organization of the diblock copolymers is driven by the tendency of the peptide segments to form well-defined tertiary structures. In contrast to conventional amphiphilic block copolymers, whose self-organization is driven by unspecific hydrophobic interactions and leads to polydisperse aggregates, it was anticipated that this approach could allow precise control over the aggregation number in aqueous solution. Circular dichroism and analytical ultracentrifugation experiments indicated that the self-organization properties of the peptide segments are retained upon conjugation of PEG, and discrete, well-defined supramolecular aggregates are formed. No evidence was found for unspecific self-organization of the diblock copolymers to large polydisperse structures, as it is the case for conventional amphiphilic block copolymers. In contrast, the self-organization of the PEG-*b*-peptide diblock copolymers is described as an equilibrium between unimeric block copolymer molecules and dimeric and tetrameric coiled coil aggregates. The relative amounts of these species depend on concentration, temperature, solvent, and the molecular weight of the PEG block.

Introduction

Depending on their architecture and chemical composition, amphiphilic block copolymers can self-assemble into micelles, vesicles, and a variety of other morphologies.[1] Under appropriate conditions, amphiphilic block copolymers can also form physically cross-linked networks or hydrogels, which can be reversibly transformed from a gel to a sol state, and vice versa.[2] These properties make amphiphilic block copolymers of interest for the development of novel materials for drug delivery[3,4] or tissue engineering applications.[5,6] The major driving force for the self-assembly of amphiphilic block copolymers are unspecific hydrophobic interactions. As a result, control over nanoscale supramolecular organization is limited, and the structure and properties of the materials can only be manipulated to a limited extent. In addition, micelles and vesicles are typically not uniform in size but possess a certain polydispersity.

Synthetic macromolecules generally are heterogeneous with respect to chain length and composition. Although this can reduce or prevent crystallization, which is advantageous for certain applications, the heterogeneous nature of synthetic macromolecules also hampers or prevents precise control of materials structure and properties at a molecular level. Proteins, on the other hand, are characterized by absolutely uniform chain lengths and a precisely defined monomer sequence (primary structure). These are two important prerequisites that allow the hierarchical self-organization of linear polypeptide chains into proteins with a precisely defined three-dimensional structure and exquisite properties. In addition to hydrophobic interactions, protein folding is also mediated by directed hydrogen-bonding interactions and electrostatic forces. Unlike synthetic macromolecules, the structure and properties of proteins are closely related to chain length and primary structure. As a result, the folding process and protein structure and properties can be precisely controlled at a molecular level.

This paper addresses the question of whether concepts of protein folding can be used to design novel macromolecular materials that self-organize in a protein-mimetic hierarchical fashion and allow precise control over nanoscale supramolecular organization and association behavior. As mentioned above, the heterogeneous nature of most synthetic macromolecules prevents precise control of structure and properties at a molecular level, which is desirable for many advanced applications in optics, electronics, and medicine. To overcome these problems, this paper will explore the conjugation of peptide sequences inspired by the protein folding process to synthetic macromolecules. If the propensity of peptide sequences to self-organize in an hierarchical fashion into well-defined higher-order structures is retained upon conjugation to a synthetic macromolecule, then this strategy may allow the development of novel macromolecular materials with unprecedented levels of structural control.

Experimental Section

Abbreviations. AUC, analytical ultracentrifugation; Ar, argon; CD, circular dichroism; DCM, dichloromethane; DHB, dihydroxybenzoic acid; DIPEA, *N*,*N*-diisopropylethylamine; DMF, *N*,*N*-dimethylformamide; Fmoc, fluorenylmethoxycar-

[†] Max Planck Institute for Polymer Research.
[‡] Johann Wolfgang Goethe-Universität.
[§] New address: École Polytechnique Fédérale de Lausanne (EPFL), Laboratoire des Polymères, Institut des Matériaux, Bâtiment MX-D, CH-1015 Lausanne, Switzerland.
* To whom correspondence should be addressed: e-mail harm-anton.klok@epfl.ch; phone ++ 41 21 693 4866; Fax ++ 41 21 693 5650.

10.1021/ma034124i CCC: $25.00
Published on Web 05/06/2003

bonyl; Gdn·HCl, guanidine hydrochloride; HBTU, *O*-benzotriazole-*N*,*N*,*N*′,*N*′-tetramethyluronium hexafluorophosphate; ^{1}H NMR, ^{1}H nuclear magnetic resonance; HOBt, *N*-hydroxybenzotriazole; MALDI−TOF MS, matrix-assisted laser desorption−ionization time-of-flight mass spectrometry; mPEG-COOH, monomethoxy poly(ethylene glycol) carboxylic acid; NMP, *N*-methyl-2-pyrrolidinone; PBS, phosphate buffered saline; PEG, poly(ethylene glycol); PyBOP, benzotriazole-1-yloxytris(pyrrolidino)phosphonium hexafluorophosphate; RP-HPLC, reversed-phase high-pressure liquid chromatography; SPPS, solid-phase peptide synthesis; [θ], mean residue ellipticity; TFE, 2,2,2-trifluoroethanol; THF, tetrahydrofuran; TFA, trifluoroacetic acid; UV/vis, ultraviolet/visible spectroscopy.

Materials. Amino acids, resins, HBTU, and HOBt were purchased from Calbiochem-Novabiochem GmbH (Schwalbach, Germany). NMP was obtained from BASF AG (Ludwigshafen, Germany). All other chemicals and reagents were acquired from Sigma Aldrich Chemie GmbH (Deisenhofen, Germany). NMP and DMF were dried over molecular sieves (4 Å) prior to use. DCM was freshly distilled from P_2O_5 before use. The synthesis of the PEG carboxylic acid derivatives (mPEG-COOH) was carried out according to a literature procedure.[7] Spectra/Por dialysis bags (made from regenerated cellulose) were purchased from Carl-Roth GmbH (Karlsruhe, Germany).

^{1}H NMR Spectroscopy. ^{1}H NMR spectra were recorded at room temperature on a Bruker Advance 250 spectrometer using the residual proton resonance of the deuterated solvent as the internal standard. For calculation of the PEG coupling yield, integrals of the well-resolved proton chemical shifts of the PEG backbone (3.54 ppm) and of the ϵ-methylene group of lysine (2.95 ppm) were compared.

MALDI−TOF Mass Spectrometry (MALDI−TOF MS). Matrix-assisted laser desorption−ionization time-of-flight (MALDI−TOF) mass spectra were recorded on a Bruker Reflex II MALDI−TOF spectrometer. Samples were dissolved in THF and mixed with the matrix DHB. Sodium trifluoroacetate was added to facilitate ionization. MALDI−TOF MS was also used to estimate the polydispersity of the PEG-*b*-peptide diblocks. The mPEG(750) conjugate and mPEG(2000) conjugate both had a polydispersity of 1.01.

Reversed-Phase High-Pressure Liquid Chromatography (RP-HPLC). RP-HPLC was performed on an Applied Biosystems Biocad Sprint workstation, using a Macherey Nagel C18 reversed-phase column (EC 250/4 NUCLEOSIL, 500 Å pore size, 5 μM particle size). Samples were eluted with a linear AB gradient from A to B over 20 min, with A consisting of 80/20 (v/v) water/acetonitrile (plus 0.1% TFA) and B of 100% acetonitrile (plus 0.1% TFA). The flow rate was 0.7 mL/min. Sample elution was monitored with a UV/vis detector at 210 nm. In all cases the purity of the peptide and the diblock copolymers was found to be ≥95%.

UV/Vis Spectroscopy. UV/vis spectra were recorded on a Perkin-Elmer Lambda 15 spectrophotometer. Molar extinction coefficients were determined by measuring samples with known concentration and deviated less than 5% from the molar extinction coefficient of tyrosine reported in the literature (ϵ_{280} = 1197 M^{-1} cm^{-1}).[8] Therefore, the literature value of the molar extinction coefficient of Tyr was used for determining sample concentrations. Concentrations were calculated according to Lambert−Beer's law.

Circular Dichroism. Circular dichroism (CD) spectra were recorded on a Jasco J-715 spectropolarimeter equipped with a Jasco PTC-348WI temperature-controlled cell. The instrument was calibrated with an aqueous solution of (+)-10-camphorsulfonic acid. Ellipticity is reported as the mean residue ellipticity ([θ], in deg cm^2 $dmol^{-1}$) and calculated as

$$[\theta] = [\theta]_{obs}(10/n_a dc)$$

where $[\theta]_{obs}$ is the ellipticity measured in millidegrees, n_a is the number of amide groups present in the main chain of the molecule, c is the total concentration of the sample in mol/L, and d is the optical path length of the cell in centimeters. Samples were dissolved in PBS (10 mM potassium phosphate (pH 7.4), 138 mM NaCl, and 2.7 mM KCl). Spectra were recorded ≥12 h after preparation of the solution. The temperature-dependent spectra were measured between 5 and 90 °C in a quartz cell with a path length of 0.1 cm. CD spectra were obtained by collecting data from 250 to 195 nm at 0.2 nm intervals, at a rate of 20 nm min^{-1}, a response time of 4 s for each point, and a bandwidth of 1 nm. Typically, 4−8 wavelength scans were averaged for a single spectrum. For thermal unfolding measurements, samples were allowed to equilibrate for 20 min at each temperature. Wavelength scans were corrected for PBS scans taken at 20 °C. Helix contents were calculated according to the method published by Chen et al.[9,10] For the maximum mean residue ellipticity value at 222 nm ($[\theta]_{222,\infty}$) of a peptide with infinite length and 100% helix content, −37 400 deg cm^2 $dmol^{-1}$ was used.[11]

Analytical Ultracentrifugation. Sedimentation equilibrium experiments were performed in a Beckman Optima XL-A analytical ultracentrifuge using Epon six-channel centerpieces with a path length of 1.2 cm in combination with an An-60Ti rotor. The rotor speed was 40 000 rpm, and the rotor temperature was 25 °C. The absorbance vs radius distributions $A(r)$ were collected at 275 nm. The experiments with peptide **1** and the diblock copolymers **2** and **3** were carried out at sample concentrations of 100 and 200 μM, corresponding to an $A^{1.2cm}_{275nm}(r)$ of 0.15 and 0.3, respectively, in PBS. The sample volume was 130 μL. The partial specific volumes were calculated to be 0.769, 0.783, and 0.796 mL/g, for samples **1**, **2**, and **3** respectively.[12] The experimental sedimentation equilibrium profiles were analyzed according to the following equation:[13−17]

$$A(r) = \sum A_i(r) = \sum A_i(r_0)\exp[iM_1(1 - \bar{\nu}\rho_0)\omega^2(r^2 - r_0^2)/2RT]$$

with i the number of protomers per oligomer, A_i the absorbance of corresponding species, M_1 the molar mass of the protomer, $\bar{\nu}$ the partial specific volume of the sample (assumed to be independent of the oligomeric state), ρ_0 the solvent density, ω the angular velocity of the rotor, r the radial position, and r_0 the fixed radial position. The evaluations were made using the computer program Discreeq.[18] They included tests for the statistical accuracy of the best fit parameters, considering the minimal increase in the sum of the squared residuals of the fit, σ, that results from one nonoptimal parameter $A_i(r_0)$; all other $A_j(r_0)$ were varied to compensate for the imposed constraint. The density of the buffer was calculated using the software Sednterp.[19]

Peptide Synthesis and Purification. Peptide synthesis was performed on an Applied Biosystems model 433A peptide synthesizer, using standard Fmoc chemistry.[20,21] The amino acid residues were used as free acids, and coupling was facilitated by the use of HBTU and HOBt. A *tert*-butyl group was chosen as a side chain protective group for the glutamic acid and tyrosine residues. Lysine side chains were protected with BOC groups. Peptide synthesis was carried out using a Rink Amide AM resin. After completion of the desired amino acid sequence, treatment of the resin-bound product with 50% TFA in DCM simultaneously cleaves the linker and removes the side chain protective groups. In this way, a peptide with a C-terminal amide group was obtained. After filtration of the resin, the solvents were evaporated to near dryness. Subsequent precipitation with cold diethyl ether gave a white powder. The peptides were purified by dialysis in, first, distilled water containing about 6 M Gdn·HCl for denaturation and NaOH for solubility (added until a clear solution is obtained) and, second, pure distilled water to remove the additional salts. Water was removed by lyophilization. Typically, after a 0.25 mmol scale synthesis, 90 mg (14%) of pure peptide was obtained as a white powder.

PEG-*b*-Peptide Synthesis. In a first step, the peptide block was prepared via SPPS as described above. Then, the resin-bound peptides were transferred to a reaction flask and coupled with the appropriate mPEG-COOH. A typical procedure is as follows: 0.5 g of resin-bound peptide was swollen in 10 mL of DMF/DCM (9/1) for 15 min. Subsequently, 4 equiv

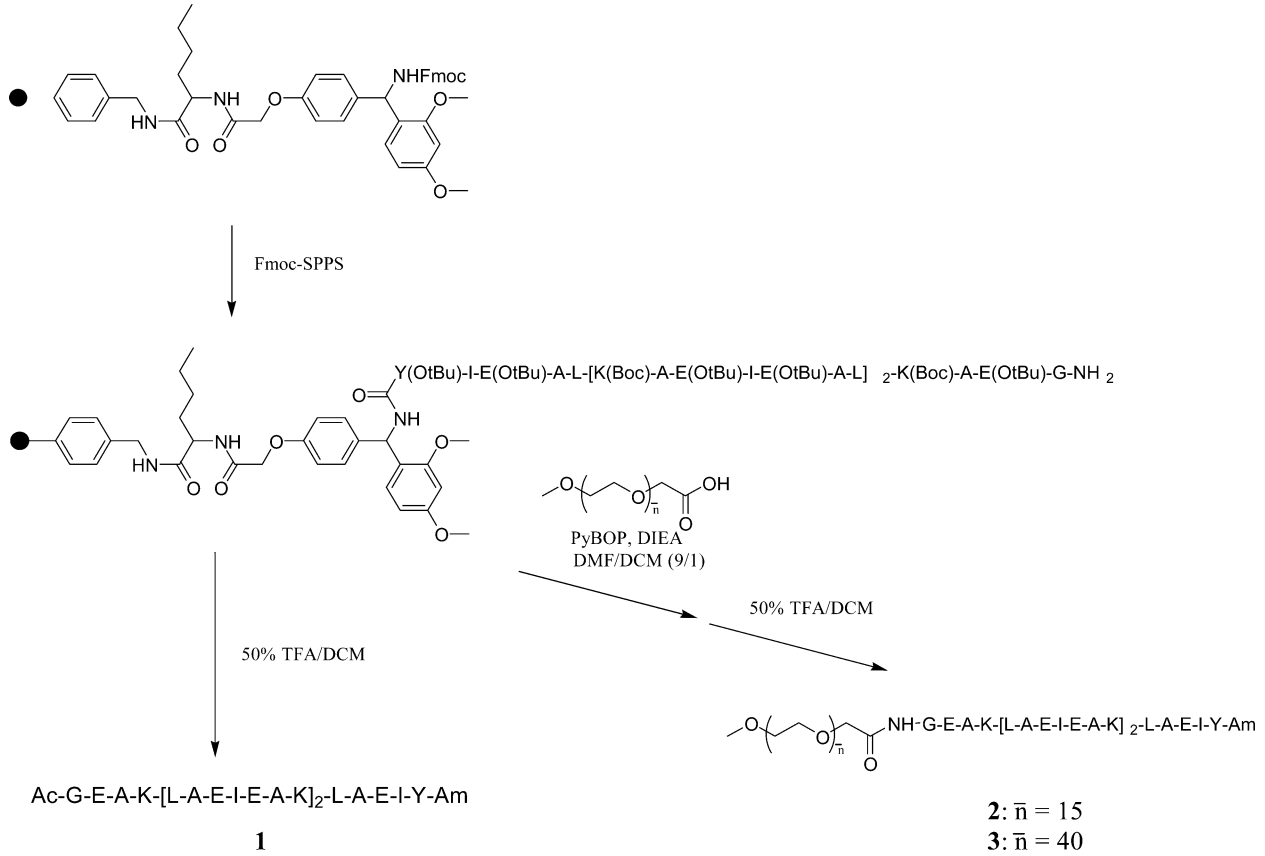

Figure 1. Synthesis of peptide **1** and diblock copolymers **2** and **3** (A, alanine; E, glutamic acid; G, glycine; I, isoleucine; K, lysine; L, leucine; Y, tyrosine).

of mPEG-COOH in DMF/DCM (9/1) was added, and the mixture was stirred for 15 min. Finally, 8 equiv of PyBOP in DMF/DCM (9/1) and 16 equiv of DIPEA were added. The mixture was stirred for 5 days at room temperature under an Ar atmosphere. Then, the mixture was filtered, and the resin was thoroughly washed with large amounts of DCM and DMF to remove unreacted PEG and other reagents. The resin was then transferred into another flask. Cleavage from the resin, precipitation, and purification were done by the same procedure as with the pure peptides to give diblock copolymers **2** and **3** as white powders in 23 and 25% yield, respectively.

Results

Design. Because of their limited size and well-defined three-dimensional structure, protein folding motifs[22] seem to be an ideal test case to explore the feasibility of the concept that was outlined in the Introduction, i.e., the question of whether the self-organization properties of peptide sequences are retained upon conjugation to synthetic macromolecules. In this contribution, we report the synthesis and self-organization of diblock copolymers composed of a peptide block based on the coiled coil motif and poly(ethylene glycol) (PEG) as the synthetic block. PEG was chosen because its water-solubility was expected to facilitate characterization of the self-organization of the diblock copolymers. Furthermore, PEG is an FDA-approved biocompatible polymer, which is advantageous for possible future medical applications.[23] A coiled coil consists of a bundle of amphiphilic, right-handed α-helices wrapped around each other at an angle of about 20° into a left-handed superhelix. This structure was first identified in tropomyosin by Francis Crick in 1953[24] and is now found in more than 200 native proteins, including fibrous proteins, muscle proteins, DNA-binding proteins, and many disease- and organ-specific autoantigens such as polymyositis and scleroderma antigens.[25] The primary structure of coiled coil forming proteins is characterized by a heptad periodicity, "*a-b-c-d-e-f-g*".[26,27] Because of the specific placement of amino acid residues in this repeat, coiled coil formation is not only driven by hydrophobic interactions but also promoted by electrostatics.

The primary structure of the peptide segment of the diblock copolymers presented in this contribution is shown in Figure 1. This amino acid sequence is derived from a de novo designed coiled coil, which was reported by Hodges and co-workers in 1994.[11] This sequence was anticipated to favor the formation of a tetrameric coiled coil.[28−30]

Synthesis and Characterization. The synthesis of the diblock copolymers is outlined in Figure 1. Independently, Kopeček and co-workers recently reported the synthesis of several structurally related block copolymers following a similar synthetic approach.[31] The α,ω-heterobifunctional PEG derivatives were prepared following the procedure published by Gehrhardt and Mutter.[7] Peptides were prepared by solid-phase peptide synthesis, using standard Fmoc chemistry.[20,21] Subsequently, the resin-bound peptides were PEGylated using a modification of the method developed by Felix and co-workers.[32] Because coupling of the first PEG chains to the resin-bound peptide sterically hinders the attachment of further PEG chains, low resin loadings (0.6−0.7 mmol/g) proved to be advantageous. Accordingly, PEGylation yields decreased significantly with increasing PEG chain length. After treatment of the resin-bound block copolymers with a trifluoroacetic acid/dichloromethane mixture, which simultaneously cleaves the product from the resin and removes the side-chain

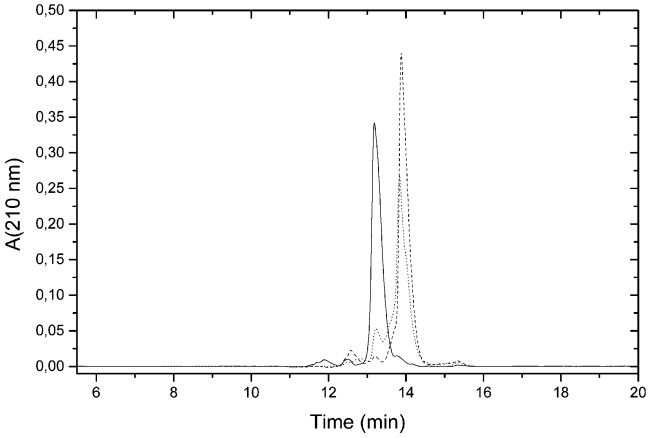

Figure 2. RP-HPLC traces of peptide **1** (—) and diblock copolymers **2** (· · ·) and **3** (- - -).

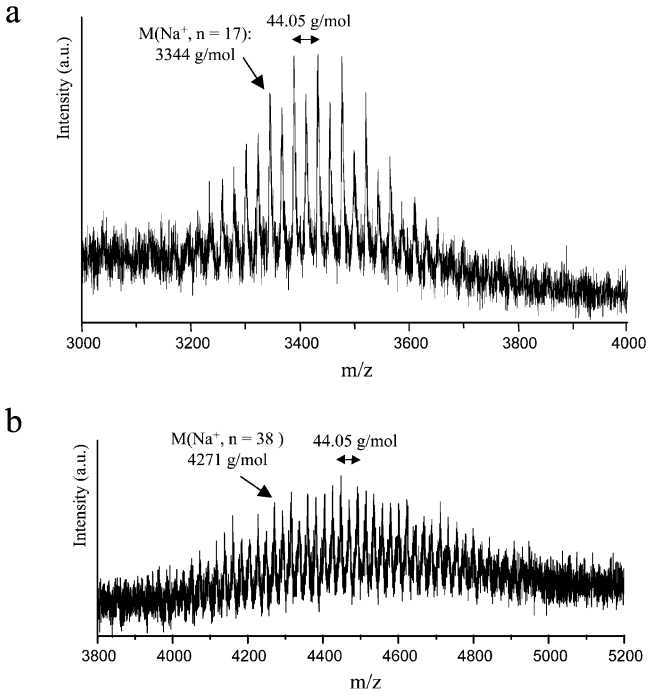

Figure 3. MALDI−TOF mass spectra of diblock copolymers **2** (a) and **3** (b).

protective groups, ^{1}H NMR showed that PEG with a molecular weight of 750 Da (mPEG-750) (n = 15) was coupled almost quantitatively, whereas the coupling yield for mPEG-2000 (n = 40) was only about 40%. The crude diblock copolymers were purified by dialysis to remove unconverted peptide.

Peptide **1** and diblock copolymers **2** and **3** were characterized by means of ^{1}H NMR spectroscopy, RP−HPLC, and MALDI−TOF MS. RP−HPLC analysis (Figure 2) of the peptide and of the diblock copolymers indicated purities higher than 95%. Each of the MALDI−TOF mass spectra in Figure 3 shows two series of peaks, which correspond to the protonated and sodium-labeled molecular ions, respectively. The distance between two neighboring peaks within one series is 44.05 Da, which is the mass of an ethylene glycol repeating unit. Note that due to the perfectly monodisperse character of the peptide segments, the MALDI−TOF mass spectra are relatively simple. Only the chain length heterogeneity of PEG contributes to the molecular weight distribution. In each of the MALDI−TOF mass spectra, a representative peak is labeled with the corresponding mass. These masses are in excellent agreement with the sum of the masses of an integer number of ethylene glycol repeats, the mass of the peptide segment and one Na^+ ion, which confirms the chemical integrity of the block copolymers.

Circular Dichroism Spectroscopy. Concentration-Dependent Experiments. To study the secondary structure of the peptide segment and the self-organization of the diblock copolymers, concentration-dependent ultraviolet CD measurements were performed (Figure 4). Within the concentration range studied (10−350 μM), the diblock copolymers and the peptide were well soluble in phosphate buffered saline (PBS) at pH 7.4. However, it was found that the solubility of the PEG-*b*-peptides was higher than the peptide itself. Whereas the diblock copolymers can be easily dissolved in pure water, the peptide itself requires additional salts (e.g., a buffer).

The spectra in Figure 4 show the characteristics of an α-helical secondary structure, i.e., negative minima at 222 and 208 nm and a positive maximum at around 195 nm. Figure 4 shows that an increase in concentration results in a decrease of the mean residue ellipticity, for both peptide **1** and the diblock copolymers **2** and **3**, which is an indication for the presence of a concentration-dependent aggregation behavior. From the CD spectra, helix contents were calculated according to the method developed by Chen et al.[9,10] using −37 400 deg cm^2 dmol^{-1} as the mean residue ellipticity for a 100% helix.[11] The helix content of the different samples is plotted as a function of concentration in Figure 5a. Figure 5b shows the concentration dependence of the ratio of mean residue ellipticities at 222 and 208 nm ($[\theta]_{222}/[\theta]_{208}$), which can be used as probe for the presence of coiled coil superstructures.[11]

In the plots in Figure 5, two regimes can be distinguished. At sufficiently high concentration, plateau values are reached, both for the helix content and for $[\theta]_{222}/[\theta]_{208}$. The helix content is highest for peptide **1** and decreases upon attachment of PEG with increasing molecular weight of the PEG block. In contrast, $[\theta]_{222}/[\theta]_{208}$ rapidly reaches a plateau value of 0.93−0.95 at ∼50 μM for all three samples. These values for $[\theta]_{222}/[\theta]_{208}$ are consistent with numbers previously reported for coiled coils.[11,33,34] Thus, the data presented in Figure 5 indicate that both peptide **1** and PEG-*b*-peptides **2** and **3** self-organize in aqueous solution via the formation of coiled coil superstructures. The difference in helix content, however, suggests that this self-organization process is not identical for all samples and may depend on the presence and molecular weight of conjugated PEG chains.

At low concentrations, extrapolation of the data shown in Figure 5a to zero indicates that the helix content of peptide **1** is smaller than that of the PEG-*b*-peptide diblock copolymers and that the helix content of the latter increases with increasing molecular weight of the PEG chain. Since at low concentrations the majority of the molecules will be present as unimers, which is supported by the rapid decrease in $[\theta]_{222}/[\theta]_{208}$ at low concentrations in Figure 5b, this suggests that PEG stabilizes the α-helical secondary structure of the peptide in unimeric state. In control experiments on mixtures of PEG and peptide no stabilization of the α-helical secondary structure was observed. The stabilization of peptide secondary structures by conjugation of PEG has been reported before.[31,35] This phenomenon

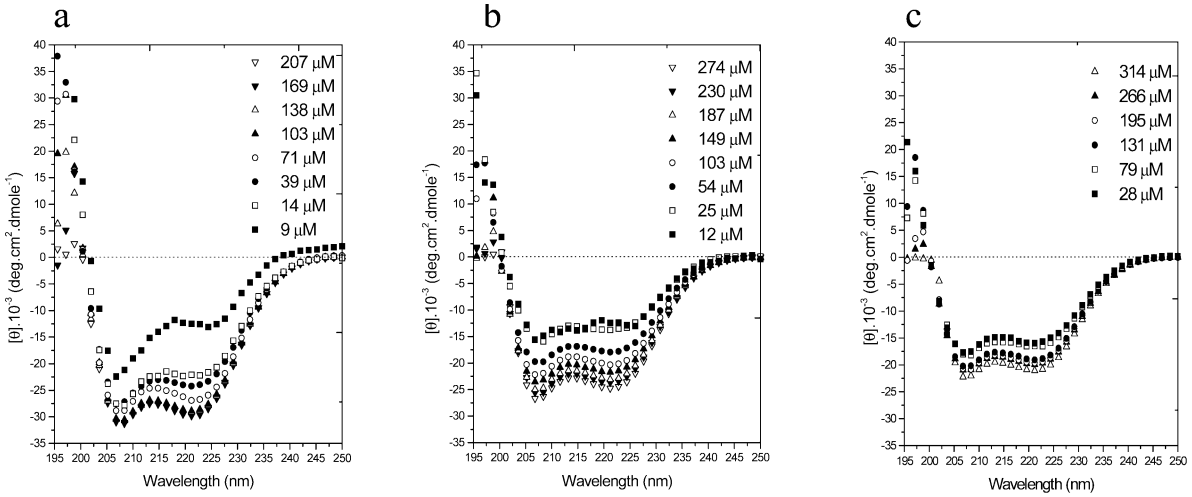

Figure 4. Concentration-dependent CD spectra of peptide **1** (a) and the diblock copolymers **2** (b) and **3** (c) in benign medium.

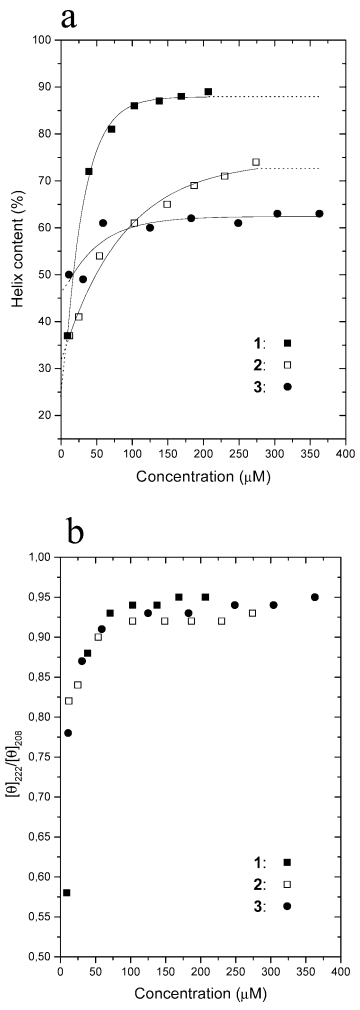

Figure 5. Plots showing (a) the concentration dependence of the helix content and (b) $[\theta]_{222}/[\theta]_{208}$ for peptide **1** and the two diblock copolymers **2** and **3** in benign medium.

may be explained by the ability of PEG to form a microhydrophobic environment which stabilizes the amphiphilic α-helical secondary structure of the peptide segment. The observed PEG chain length dependence, however, has not been reported before but may be attributed to an increase in size of the hydrophobic microdomain with increasing molecular weight of the PEG block.

Table 1. Comparison of Aggregation Behavior in Benign Medium and in Aqueous Solutions Containing 50% TFE

		benign medium		50% TFE	
compd	concn[a] (μM)	helix content (%)	$[\theta_{222}]/[\theta_{208}]$	helix content (%)	$[\theta_{222}]/[\theta_{208}]$
1	100	86	0.94	91	0.84
	200	89	0.95	91	0.83
2	100	62	0.91	85	0.82
	200	67	0.93	78	0.83
3	100	46	0.88	81	0.80
	200	55	0.90	56	0.81

[a] Concentrations are ±10 μM.

TFE Addition. The self-organization of peptide **1** and PEG-*b*-peptides **2** and **3** was further investigated by CD measurements in aqueous solutions containing 50% TFE. At low concentrations (5−15% v/v), TFE (2,2,2-trifluoroethanol) is known to promote helix formation in peptides that are partially unstructured in benign medium.[36] Addition of 50% TFE to aqueous solutions of coiled coils, which already possess a nearly full helix content, however, causes dissociation of coiled coils into single-stranded α-helices and, in addition, increases the helicity of the remaining partially unstructured segments.[33,37] The transition from coiled coil tertiary structures to single-stranded α-helices is accompanied by a decrease in $[\theta]_{222}/[\theta]_{208}$.

Results of the quantitative analysis of CD spectra of peptide **1** and diblock copolymers **2** and **3** recorded in 50% TFE at two different sample concentrations are shown in Table 1. The data in Table 1 show that addition of 50% TFE results in a decrease of $[\theta]_{222}/[\theta]_{208}$ as would be expected for the dissociation of coiled coils in single-stranded α-helices. This decrease in $[\theta]_{222}/[\theta]_{208}$ is accompanied by an increase in helix content. This suggests that in benign medium the self-organization of the diblock copolymers and peptide **1** can be described as an equilibrium between coiled coil aggregates and unimers with an unordered or partially ordered peptide segment.

Temperature-Dependent Experiments. Temperature-dependent CD spectra of diblock copolymer **2** at a concentration of 187 μM in benign medium are shown in Figure 6. The helix content and $[\theta]_{222}/[\theta]_{208}$, which can be determined from these spectra, are plotted as a function of temperature in Figure 7 for all compounds discussed in this paper. High sample concentrations were used to ensure a high coiled coil content.

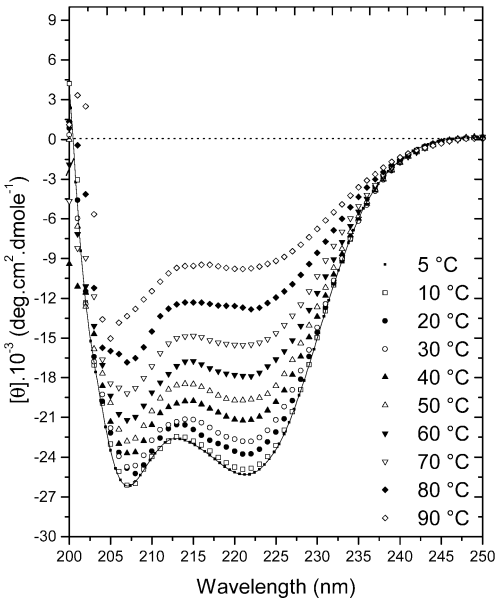

Figure 6. Temperature-dependent CD spectra of diblock copolymer **2** at 187 μM showing the fast and reversible thermal denaturation in benign medium. The solid line is the CD curve after rapid cooling (over a period of 10 min) from 90 to 5 °C.

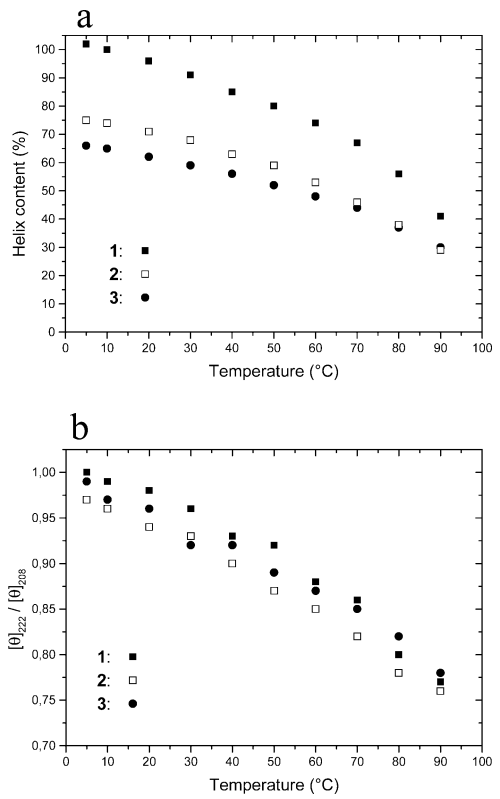

Figure 7. Plots of (a) the helix content and (b) $[\theta]_{222}/[\theta]_{208}$ of peptide **1** (169 μM) and the two diblock copolymers **2** (187 μM) and **3** (249 μM) vs temperature.

The data in Figure 6 and Figure 7 provide further insight into the self-organization of **1**−**3**. First of all, the helix content and $[\theta]_{222}/[\theta]_{208}$ decrease with increasing temperature, which suggests a gradual dissociation ("denaturation/unfolding") of coiled coil aggregates into partially ordered unimers. The smooth change in helix content with temperature indicates folding/unfolding takes place in a cooperative fashion. As shown in Figure 6, thermal denaturation is fully reversible, and refolding is complete within 10 min. A final interesting result from the temperature-dependent CD experiments is the difference in loss of helix content upon heating between the different samples. Figure 7a shows that heating peptide **1** from 5 to 90 °C results in a 60% loss of helix content, whereas block copolymers **2** and **3** only lose 45% and 30%, respectively, of their initial helix content over this temperature range. These observations may be explained by the stabilizing influence of the PEG block on the secondary structure of the peptide segment, which was already proposed before. In line with the results from the concentration-dependent experiments there seems to be a PEG molecular weight dependence, with longer PEG blocks attached, resulting in a smaller loss of helix content of the peptide.

Table 2. Concentration Dependence of the Unimer (U), Dimer (D), Tetramer (T), and Octamer (O) Content, Estimated from Sedimentation Equilibrium Analysis

compd	concn (μM)	U content (%)[a]	D content (%)[a]	T content (%)[a]	O content (%)[a]
1	100	0 (0−27)	53 (13−56)	40 (37−55)	0
	200	9 (3−14)	38 (29−47)	55 (51−59)	small
2	100	40 (29−51)	18 (0−37)	42 (34−51)	0
	200	25 (20−29)	27 (20−35)	48 (45−52)	0
3	100	42 (37−48)	39 (30−48)	19 (15−23)	0
	200	40 (37−43)	36 (31−42)	25 (22−28)	0

[a] Numbers representing the most probable figure (range) for the oligomer content. The asymmetry of the limits of error is due to the asymmetry of the $\sigma(A)$ curves (curves not shown).

Analytical Ultracentrifugation. To complement the CD studies, analytical ultracentrifugation (AUC) experiments were performed under identical conditions. Sedimentation equilibrium analysis of peptide **1** and diblock copolymers **2** and **3** indicated that the self-organization of all compounds can be best interpreted in terms of a unimer (U), dimer (D), tetramer (T) equilibrium. An estimate for the relative amounts of each of these species at 100 and 200 μM is presented in Table 2. It is obvious from the table that the PEG segment of the copolymer hinders aggregation, leading to strongly increased unimer contents and less tetramer. In addition, at higher concentration, there is a slight trend toward the formation of the larger tetramer aggregates for all three compounds. At 200 μM, peptide **1** contained a few percent of octamers. In all other samples, however, the presence of significant amounts of aggregates larger than tetramers could be ruled out.

Discussion

The results of the CD and AUC experiments can be summarized in the model shown in Figure 8. The self-organization of the PEG-*b*-peptide diblock copolymers can be described as an equilibrium between discrete unimeric, dimeric, and tetrameric supramolecular species. The tendency of the peptide segments to form coiled coil superstructures provides the driving force for this process. Qualitatively, the behavior of peptide **1** and diblock copolymers **2** and **3** is identical. Quantitatively, however, there are several significant differences between peptide **1** and diblock copolymers **2** and **3**, especially with respect to the relative amounts of the different supramolecular aggregates that are formed and the thermal stability of these species. To discuss these similarities and differences, it is useful to distinguish between a high and a low concentration regime.

At sufficiently high concentrations, the CD spectra suggested the self-organization of **1**, **2**, and **3** via the formation of coiled coil superstructures. These observa-

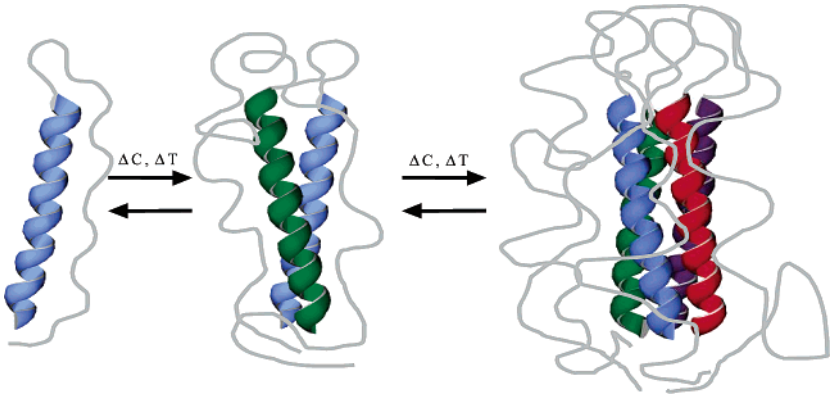

Figure 8. Proposed model for the self-assembly of the PEG-*b*-peptide diblock copolymers **2** and **3**.

tions were supported by the results from AUC. Sedimentation equilibrium analysis of peptide **1** indicated that this peptide self-organizes mainly into discrete tetrameric aggregates, which was also anticipated on the basis of the amino acid sequence. Sedimentation equilibrium analysis of **2** and **3** also revealed the formation of discrete tetrameric supramolecular aggregates. However, in these cases the relative amount of tetramers was reduced in comparison with peptide **1**, and larger fractions of dimers and, in particular, unimers were found. Interestingly, the shift toward a smaller fraction of tetramers and increasing amounts of dimers and unimers becomes more pronounced upon increasing the molecular weight of the PEG block. These observations are in agreement with the decrease in helix content which was found by CD spectroscopy upon conjugation of PEG to peptide **1** and upon increasing the molecular weight of the PEG block. Apparently, the presence of the PEG block sterically hinders the formation of tetrameric aggregates and shifts the equilibrium depicted in Figure 8 toward the side of unimeric species. In line with the increase in helix content which was observed in the CD experiments, the analytical ultracentrifugation investigations revealed an increase in the relative amount of the larger aggregates at higher concentration. Furthermore, temperature-dependent CD experiments revealed that attachment of PEG significantly enhances the stability of the coiled coil superstructures toward thermal denaturation. This may be explained by the amphiphilic character of PEG, which allows the formation of an hydrophilic, protective shell around an hydrophobic interior stabilizing the peptide secondary structure. This explanation is supported by the observed increase in thermal stability of the coiled coil aggregates with increasing length of the PEG block. The stabilizing influence of PEG on peptide secondary structures was not only reflected in the enhanced thermal stability of the supramolecular aggregates but also revealed, though in a different manner, during concentration-dependent CD experiments. Extrapolation to zero concentration, i.e., to a hypothetical state where all PEG-*b*-peptides are unimeric and the peptide segments are instable because of their intrinsic amphiphilicity, indicated that the helix contents of the (unimeric) peptide segments in the diblock copolymers were higher than that of peptide **1** and increased with increasing molecular weight of the PEG block. These results provide a further indication for the formation of a protective and secondary structure stabilizing shell around the peptide segment.

Conclusions

In this paper we have reported the synthesis and self-organization of two novel PEG-*b*-peptide diblock copolymers, which contain peptide sequences inspired by the coiled coil protein folding motif. Unlike most water-soluble block copolymers, the PEG-*b*-peptide diblock copolymers are not amphiphilic (both PEG and peptide are amphiphilic), and their self-organization is not only driven by hydrophobic interactions. Instead, the self-organization of the PEG-*b*-peptide diblock copolymers is mediated by the propensity of the peptide segments to form well-defined tertiary structural motifs, which was anticipated to allow enhanced control over size and shape of the supramolecular aggregates in comparison with conventional amphiphilic block copolymers. CD and AUC experiments indicated that the self-organization properties of the peptide segments are retained upon conjugation to PEG. In contrast to conventional amphiphilic block copolymers, which form polydisperse micelles and vesicles, the PEG-*b*-peptide block copolymers self-organize into discrete, well-defined supramolecular aggregates. Qualitatively, these observations agree with the results of an independent study of a structurally related class of block copolymers by Kopeček et al. which was recently published.[31] The self-organization of the diblock copolymers discussed in the present contribution can be described as an equilibrium between unimeric diblock copolymer molecules and dimeric and tetrameric aggregates, which are held together by organization of two or four peptide segments into coiled coil superstructures. In comparison with the pure peptide, conjugation of PEG sterically hampers the formation of tetrameric aggregates and shifts the equilibrium toward smaller dimeric aggregates and unimers. Conjugation of PEG, however, results in an increased stability toward thermal denaturation, presumably via the formation of a PEG shell around the coiled coil superstructures. The ability to transfer the self-organization properties of specific peptide sequences to hybrid block copolymers, as it has been demonstrated in this contribution, may allow the development of novel macromolecular materials characterized by unprecedented hierarchical nanoscale order. Accurate control of structure and organization at the nanometer level is advantageous for many advanced applications in for example optics, electronics, and medicine.

Acknowledgment. This work was supported by the Stiftung Stipendien Fonds des Verbandes der Chemischen Industrie, the Bundesministerium für Bildung und Forschung, the International Max Planck Research

School (G.V.), and the Deutsche Forschungsgemeinschaft (Emmy Noether-Program KL 1049/2) (H.-A.K.). BASF AG (Ludwigshafen, Germany) is acknowledged for donating NMP. The authors are grateful to Prof. K. Müllen for his continuous support and interest in this work, to Prof. D. Schubert for helpful advise and suggestions, and to Dr. C. Clark for his help with the graphics.

References and Notes

(1) Förster, S.; Plantenberg, T. *Angew. Chem., Int. Ed.* **2002**, *41*, 688−714.
(2) Bromberg, L. E.; Ron, E. S. *Adv. Drug Delivery Rev.* **1998**, *31*, 197−221.
(3) Rösler, A.; Vandermeulen, G. W. M.; Klok, H.-A. *Adv. Drug Delivery Rev.* **2001**, *53*, 95−108.
(4) Kabanov, A. V.; Alakhov, V. Y. *Crit. Rev. Ther. Drug Carrier Syst.* **2002**, *19*, 1−72.
(5) Jeong, B.; Kim, S. W.; Bae, Y. H. *Adv. Drug Delivery Rev.* **2002**, *54*, 37−51.
(6) Otsuka, H.; Nagasaki, Y.; Kataoka, K. *Curr. Opin. Colloid Interface Sci.* **2001**, *6*, 3−10.
(7) Gehrhardt, H.; Mutter, M. *Polym. Bull. (Berlin)* **1987**, *18*, 487−492.
(8) *Bioanalytik*; Lottspeich, F., Zorbas, H., Eds.; Spektrum Akademischer Verlag GmbH: Heidelberg, 1998.
(9) Chen, Y.-H.; Yang, J. T.; Martinez, H. M. *Biochemistry* **1972**, *11*, 4120−4131.
(10) Chen, Y.-H.; Yang, J. T.; Chau, K. H. *Biochemistry* **1974**, *13*, 3350−3359.
(11) Su, J. Y.; Hodges, R. S.; Kay, C. M. *Biochemistry* **1994**, *33*, 15501−15510.
(12) Durchschlag, H. In *Thermodynamic Data for Biochemistry and Biotechnology*; Hinz, H.-J., Ed.; Springer-Verlag: Berlin, 1986; pp 45−128.
(13) Schubert, D.; Schuck, P. *Prog. Colloid Polym. Sci.* **1991**, *86*, 12−22.
(14) Schuck, P.; Legrum, B.; Passow, H.; Schubert, D. *Eur. J. Biochem.* **1995**, *230*, 806−812.
(15) Musco, G.; Tziatzios, C.; Schuck, P.; Pastore, A. *Biochemistry* **1995**, *34*, 553−561.
(16) Collinson, I.; Breyton, C.; Duong, F.; Tziatzios, C.; Schubert, D.; Or, E.; Rapoport, T.; Kühlbrandt, W. *EMBO J.* **2001**, *20*, 2462−2471.
(17) Tziatzios, C.; Precup, A. A.; Weidl, C.; Schubert, U. S.; Schuck, P.; Durchschlag, H.; Mächtle, W.; van den Broek, J. A.; Schubert, D. *Prog. Colloid Polym. Sci.* **2002**, *119*, 24−30.
(18) Schuck, P. *Prog. Colloid Polym. Sci.* **1994**, *94*, 1−13.
(19) Laue, T. M.; Shah, B. D.; Ridgeway, T. M.; Pelletier, S. L. In *Analytical Ultracentrifugation in Biochemistry and Polymer Science*; *Computer-Aided Interpretation of Analytical Sedimentation Data for Proteins*; Harding, S. E., Rowe, A. J., Horton, J. C., Eds.; The Royal Society of Chemistry: Cambridge, UK, 1992; pp 90−125.
(20) *Fmoc Solid-Phase Peptide Synthesis*; Chan, W. C., White, P. D., Eds.; Oxford University Press: Oxford, 2000.
(21) Fields, G. B.; Noble, R. L. *Int. J. Peptide Protein Res.* **1990**, *35*, 161−214.
(22) *Introduction to Protein Structure*, 2nd ed.; Branden, C., Tooze, J., Eds.; Garland Publishing: New York, 1999.
(23) *Poly(ethylene glycol)−Chemistry and Biological Applications;* Harris, J. M., Zalipsky, S., Eds.; ACS Symposium Series 680; American Chemical Society: Washington, DC, 1997.
(24) Crick, F. H. C. *Acta Crystallogr.* **1953**, *6*, 685−697.
(25) Lupas, A. *Trends Biochem. Sci.* **1996**, *21*, 375−382.
(26) Hodges, R. S.; Sodek, J.; Smillie, L. B.; Jurasek, L. *Cold Spring Harbor Symp. Quantum Biol.* **1972**, *37*, 299−310.
(27) Sodek, J.; Hodges, R. S.; Smillie, L. B.; Jurasek, L. *Proc. Natl. Acad. Sci. U.S.A.* **1972**, *69*, 3800−3804.
(28) Harbury, P. B.; Kim, P. S.; Alber, T. *Nature (London)* **1994**, *371*, 80−83.
(29) Lovejoy, B.; Choe, S.; Cascio, D.; McRorie, D. K.; DeGrado, W. F.; Eisenberg, D. *Science* **1993**, *259*, 1288−1293.
(30) Harbury, P. B.; Zhang, T.; Kim, P. S.; Alber, T. *Science* **1993**, *262*, 1401−1407.
(31) Pechar, M.; Kopečková, P.; Joss, L.; Kopeček, J. *Macromol. Biosci.* **2002**, *2*, 199−206.
(32) Lu, Y.-A.; Felix, A. M. *Peptide Res.* **1993**, *6*, 140−146.
(33) Lau, S. Y. M.; Taneja, A. K.; Hodges, R. S. *J. Biol. Chem.* **1984**, *259*, 13253−13261.
(34) Zhou, N. E.; Kay, C. M.; Hodges, R. S. *J. Biol. Chem.* **1992**, *267*, 2664−2670.
(35) Harada, A.; Cammas, S.; Kataoka, K. *Macromolecules* **1996**, *29*, 6183−6188.
(36) Cammers-Goodwin, A.; Allen, T. J.; Oslick, S. L.; McClure, K. M.; Lee, J. H.; Kemp, D. S. *J. Am. Chem. Soc.* **1996**, *118*, 3082−3090.
(37) Chitra, R.; Smith, P. E. *J. Chem. Phys.* **2001**, *114*, 426−435 and references therein.

MA034124I